

# AIM 2025 challenge on Inverse Tone Mapping Report: Methods and Results

Chao Wang\*      Francesco Banterle \*      Bin Ren\*      Radu Timofte\*      Xin Lu  
 Yufeng Peng      Chengjie Ge      Zhijing Sun      Ziang Zhou      Zihao Li      Zishun Liao  
 Qiyu Kang      Xueyang Fu      Zheng-Jun Zha      Zhijing Sun      Xingbo Wang      Kean Liu  
 Senyan Xu      Yang Qiu      Yifan Ding      Gabriel Eilertsen      Jonas Unger      Zihao Wang  
 Ke Wu      Jinshan Pan      Zhen Liu      Zhongyang Li      Shuaicheng Liu  
 S.M Nadim Uddin

## Abstract

*This paper presents a comprehensive review of the AIM 2025 Challenge on Inverse Tone Mapping (ITM). The challenge aimed to push forward the development of effective ITM algorithms for HDR image reconstruction from single LDR inputs, focusing on perceptual fidelity and numerical consistency. A total of 67 participants submitted 319 valid results, from which the best five teams were selected for detailed analysis. This report consolidates their methodologies and performance, with the lowest PU21-PSNR among the top entries reaching 29.22 dB. The analysis highlights innovative strategies for enhancing HDR reconstruction quality and establishes strong benchmarks to guide future research in inverse tone mapping.*

## 1. Introduction

Inverse Tone Mapping (ITM) aims to reconstruct high dynamic range (HDR) images from single low dynamic range (LDR) inputs. This process involves several key steps, including de-quantization, de-contouring, linearization, dynamic range expansion, completion of overexposed and underexposed regions, and color gamut extension [7]. Inverse Tone Mapping (ITM) is essential for displaying legacy LDR content on HDR devices, enabling existing images and videos to benefit from the wider dynamic range and color gamut of modern displays. With the rapid adoption of HDR technology, ITM has gained importance not only in consumer entertainment but also in applications such as digital

archiving, photography, gaming, and VR/AR [8, 42, 76].

Before the rise of deep learning, ITM methods were primarily model-driven [1, 4–6, 18, 38, 55–57, 59, 63]. These approaches focused on linearization and dynamic range expansion using analytical tone-mapping functions or inverse camera response models. While they perform adequately for high-quality LDR inputs with minimal saturation or quantization artifacts, they fail to reconstruct missing information in heavily overexposed or underexposed regions.

With the advent of deep learning, ITM has significantly advanced through data-driven models that can restore lost details and hallucinate plausible content in saturated areas. Existing learning-based methods can be broadly divided into direct and indirect approaches. Direct methods reconstruct HDR images from LDR inputs in an end-to-end manner. HDRCNN [22] pioneered this direction with a VGG-based [69] CNN and a luminance-reflectance decomposition loss to improve reconstruction quality. [54] introduced ExpandNet, a multi-branch network capturing local, medium, and global context to mitigate U-Net artifacts. MaskHDR[67] employed feature masks inspired by partial convolutions [44] to emphasize unsaturated regions, while SingleHDR [45] decomposed ITM into subproblems such as de-quantization and linearization, using specialized sub-networks for each. [79] designed a two-stream architecture balancing saturated and unsaturated regions, and [19] adopted intrinsic decomposition to separately reconstruct shading and albedo, ensuring color fidelity.

Indirect methods first synthesize virtual exposure stacks from the input and then merge them into HDR. DrTMO [23] combined a 2D U-Net encoder with a 3D U-Net [13] decoder to generate exposure sequences, followed by merging based on [17]. [40] adapted the EDSR architecture [43] for cascaded exposure generation, later enhanced by recursive designs to reduce parameters [41]. [39] enforced feature consistency across exposures using representation loss, and [80] introduced Swin-Transformer [46, 61, 62] for long-range dependency modeling with an end-to-end fusion.

\* C. Wang (winchao1984@gmail.com, MPI-Info, Germany & Peng Cheng Laboratory, China), F. Banterle (francesco.banterle@isti.cnr.it, ISTI-CNR, Italy), B. Ren (bin.ren@unitt.it, University of Pisa, & University of Trento, Italy), and R. Timofte (Radu.Timofte@uni-wuerzburg.de, University of Würzburg, Germany) were the challenge organizers, while the other authors participated in the challenge.

Appendix A contains the authors' teams and affiliations.

AIM 2025 webpage: <https://cvlai.net/aim/2025/>.

Beyond static images, ITM has been extended to video. [36] synthesized training data from HDR videos and proposed a two-branch network that jointly addresses ITM and super-resolution by separating low and high frequency components, further improved with GAN regularization [37]. [29] designed a context-aware hierarchical module for modeling global-local relationships, enhancing temporal consistency. [34] treated adjacent frames as implicit multi-exposure inputs, combining them through a pyramid-based optical flow alignment. [8] further advanced this by exploiting inter-frame similarity to transfer details from unsaturated frames to saturated ones without supervision.

Recently, generative models have also been introduced into ITM, opening new possibilities for detail synthesis and enhanced visual realism. These approaches leverage generative priors to hallucinate missing content and improve reconstruction quality, representing a promising direction for future research. GlowGAN [74] learns HDR generation from unlabeled LDR data via a differentiable camera model and employs GAN inversion [60, 68, 71, 77] for ITM, reducing dependency on HDR ground truth. Building on this concept, [9] and [27] extend it to diffusion models, enabling multi-exposure synthesis and HDR reconstruction without fine-tuning, marking a paradigm shift toward generative modeling for ITM. Moreover, LEDiff [76] finetunes a pretrained Stable Diffusion model [64] on a small HDR dataset, greatly improving the reconstruction of overexposed and underexposed regions and enabling photorealistic HDR synthesis.

As HDR displays become increasingly prevalent and the demand for high-quality visual content rises, ITM plays a critical role in bridging the gap between existing LDR media and emerging HDR standards. Efficient and accurate ITM solutions not only enable improved visual experiences but also set the foundation for advanced applications such as HDR video streaming, immersive media, and content remastering, but also ensure long-term compatibility and accessibility of visual content across diverse devices and display technologies.

In collaboration with the Advances in Image Manipulation (AIM 2025) workshop, we organize the AIM 2025 Challenge on Inverse Tone Mapping. The goal is to reconstruct high-quality HDR images from single-exposure LDR inputs, with emphasis on faithful dynamic range expansion and detail recovery. Participants optimize for PU21-PSNR and PU21-SSIM to ensure both radiometric accuracy and perceptual quality. The challenge promotes practical and innovative solutions, establishes standardized evaluation protocols, and advances the development of robust HDR reconstruction systems. For context, the lowest scores achieved on the development and test sets are 29.83 / 29.22 for PU21-PSNR and 0.85 / 0.85 for PU21-SSIM, respectively.

This challenge is one of the AIM 2025 workshop associated challenges on: high FPS non-uniform motion deblurring [14], rip current segmentation [21], inverse tone mapping [75], robust offline video super-resolution [35], low-light raw video denoising [78], screen-content video quality assessment [66], real-world raw denoising [15], perceptual image super-resolution [16], efficient real-world deblurring [26], 4K super-resolution on mobile NPUs [30], efficient denoising on smartphone GPUs [32], efficient learned ISP on mobile GPUs [31], and stable diffusion for on-device inference [33]. Descriptions of the datasets, methods, and results can be found in the corresponding challenge reports.

## 2. AIM 2025 Inverse Tone Mapping Challenge

### 2.1. Overview

The primary targets of the challenge are:

- Promoting research in the area of single-image inverse tone mapping for HDR reconstruction.
- Facilitating fair and comprehensive comparisons between the efficiency and accuracy of various ITM methods.
- Providing a platform for academic and industrial participants to engage, exchange ideas, and foster collaborations in advancing HDR technologies.

Specifically, the competition addresses four key tasks:

- (i) **Compression artifact removal:** Many LDR images are stored in compressed formats such as JPEG. This introduces blocking and similar artifacts that require elimination.
- (ii) **Denoising:** Noise often appears in dark regions of LDR images due to sensor limitations. Effective denoising is therefore essential.
- (iii) **Linearization and dynamic range expansion:** LDR images typically use nonlinear compression within a limited range. HDR reconstruction demands reversing this process and expanding the range.
- (iv) **Completion of over/under exposed regions:** Overexposed highlights and underexposed shadows result in missing information. Restoring these regions is crucial for high-quality HDR output.

### 2.2. Dataset

We collect HDR images from several publicly available datasets [25, 28, 45, 58, 72] and evaluate performance on the benchmark from [24], and on additional unpublished samples. Since these HDR images are stored in relative luminance values, we apply normalization prior to processing, following the recommendation in [76]. To synthesize LDR data, we first estimate the maximum valid exposure range of each HDR image using the method described in [2], then sample exposures within this range and inject noise into the sampled images. Pixel values are subsequently clipped to

<https://www.cvlai.net/aim/2025/>

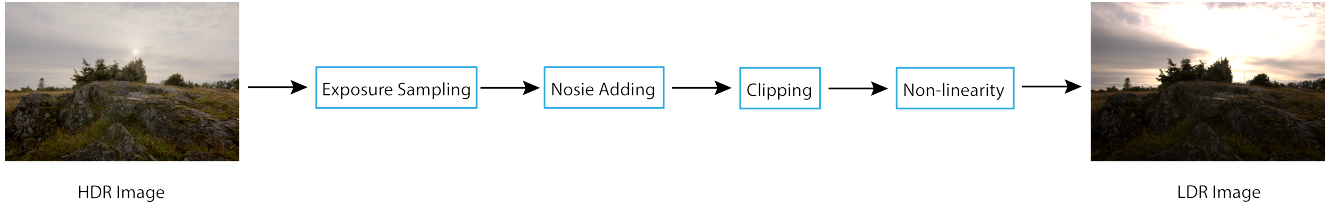


Figure 1. ITM Dataset creation pipeline.

the range  $[0, 1]$ . Following [22], we sample a camera response function from clustered CRF databases and apply it to achieve nonlinearity, thereby simulating the behavior of a real imaging pipeline. Finally, the processed images are stored as 8-bit JPEG LDR images. The overall dataset preparation pipeline is illustrated in Figure 1.

### 2.3. Challenge Description

The objective of this challenge is to reconstruct high dynamic range (HDR) images from single low dynamic range (LDR) inputs. The dataset consists of paired LDR-HDR images generated from real HDR content through tone mapping, exposure sampling, and noise simulation. The training set contains approximately 19,000 LDR-HDR pairs at a resolution of  $256 \times 256$ , while the validation and test sets include 100 images each at  $512 \times 512$  resolution.

#### Challenge phases:

(1) *Development and validation phase:* Participants are provided with the full training set and the validation set. The validation data serve for online evaluation, where participants upload HDR reconstructions to the evaluation server and receive PU21-PSNR and PU21-SSIM scores. Baseline code and evaluation scripts are available to assist in model development and ensure reproducibility.

(2) *Testing phase:* During the final test phase, participants receive only the 100 LDR test images, with the corresponding HDR ground truths kept hidden for unbiased evaluation. Participants must submit their reconstructed HDR outputs to the evaluation server and provide both their code and a factsheet. The organizers verify and execute the submitted code to compute final scores, which are shared with participants after the challenge concludes.

**Evaluation Metrics:** Performance is evaluated via perceptually uniform metrics specifically designed for HDR image quality assessment, namely PU21-PSNR and PU21-SSIM, as suggested in [3]. To reduce dataset bias, we apply camera response curve correction following the approach in [28].

In addition, participants are encouraged to report the number of parameters and inference runtime. A U-Net-based baseline model is provided for reference, achieving PU21-PSNR of 27.23 and PU21-SSIM of 0.91 on the validation set.

Table 1. PU21-PSNR and PU21-SSIM results of the challenge on the test set.

Team	PU21-PSNR (dB)	PU21-SSIM
ToneMapper	<b>34.49</b>	<b>0.95</b>
HDRer	34.39	0.95
LiU_CGIP	34.33	0.95
UESTC-ITM	34.06	0.94
Jowgik (DITM)	33.64	0.94
NJ Challenger	29.22	0.85

### 3. Challenge Results

The AIM 2025 Challenge on Inverse Tone Mapping attracted 69 participants and recorded a total of 319 submissions. Six teams submitted final results. All entries were evaluated based on PU21-PSNR and PU21-SSIM, which reflect both radiometric accuracy and perceptual quality in HDR reconstruction, see Table 1. The best performance on the test set was achieved by **ToneMapper**, reaching a PU21-PSNR of 34.49 dB and PU21-SSIM of 0.95. **HDRer** and **LiU\_CGIP** closely followed with PSNRs of 34.39 dB and 34.33 dB, respectively, both also reaching an SSIM of 0.95. At the lower end, **NJ Challenger** recorded the minimum scores with 29.22 dB in PSNR and 0.85 in SSIM, demonstrating the difficulty of restoring severely saturated or underexposed regions. Across all teams, the PU21-PSNR scores ranged from 29.83 to 34.58 dB on the development set and 29.22 to 34.49 dB on the test set; PU21-SSIM ranged from 0.85 to 0.95 on both sets, indicating relatively tighter variance in perceptual structure despite broader fidelity differences.

**ToneMapper** adopts a NAFNet-based architecture designed for efficient multi-scale image restoration. Its key innovation lies in the use of regularization-enhanced training, inspired by EEDTP, which improves generalization under diverse LDR degradations. The team employed a three-stage training scheme with progressively increasing patch sizes and decreasing learning rates, trained entirely on the official dataset. The method balances performance and efficiency, with moderate complexity (27.18M parameters, 4.84 GFLOPs) and high-quality output.

**HDRer** builds on the same NAFNet backbone but intro-

duces diffusion-based data augmentation to diversify training inputs. Instead of architectural changes, the method generates additional synthetic LDR scenes to mimic varied dynamic range conditions. These are then incorporated into the same three-stage training pipeline as ToneMapper. The approach reduces model size (15.51M parameters) while achieving nearly equivalent performance, demonstrating the effectiveness of data-centric strategies for ITM.

**LiU\_CGIP** proposes a diffusion-based generative model using the Refusion framework. It formulates inverse tone mapping as a score-based restoration problem in the PU21 space. A modified NAFNet backbone estimates score functions across time steps within a stochastic differential equation framework. Extensive external HDR data (4,000 images) is used for training, with additional SSIM-regularized loss terms improving perceptual consistency. Although computationally demanding (131.4M parameters, 253.6 GFLOPs, 6s per image), the model achieves near state-of-the-art performance and provides valuable insights into the challenges of restoring saturated regions.

**NJ Challenger** presents a modular approach that reverses the camera imaging pipeline. It decomposes ITM into 3 stages: dequantization, linearization, and hallucination. Each stage is handled by a dedicated network (U-Net, ResNet18, and VGG-based encoder-decoder), trained separately with specialized loss functions. The method incorporates prior knowledge such as CRF constraints and perceptual losses from pretrained VGG features. While conceptually well-grounded, the method underperforms in both PSNR and SSIM, highlighting the challenge of modeling each stage independently in complex HDR reconstructions.

**UESTC-ITM** proposes a dual-branch framework called ITMFlow that fuses generative modeling and deterministic regression. The first branch uses conditional flow matching to reconstruct PU21-encoded HDR from noisy LDR inputs, while the second branch employs a hybrid CNN+ViT architecture optimized for PU metrics. Both branches are trained independently and fused at test time via averaging. Despite using only the official dataset, the method achieves high quantitative and perceptual performance (34.06 dB PSNR, 0.94 SSIM) with manageable complexity (69.79M parameters, 1.4s per image), demonstrating the effectiveness of hybrid architectures.

**Jowgik (DITM)** introduces a progressive pipeline comprising BitRecoverNet, BitExpansionNet, and DetailEnhancementNet. The model first recovers quantized bits and decomposes the image into exposure-based components before gradually expanding the dynamic range and refining details. Multiple loss terms, including  $\mu$ -law compressed L1, PU-domain SSIM, and patch-wise histogram matching learning at various stages. With only 1.97M parameters and 25.64 GFLOPs, the model offers an efficient solution with strong visual quality and competitive test scores

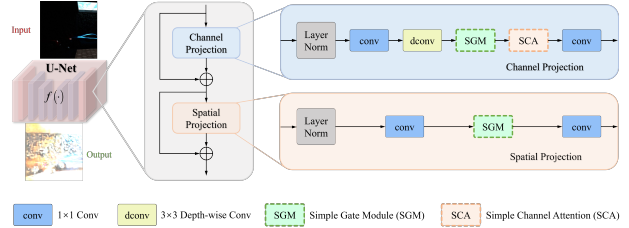


Figure 2. *ToneMapper*'s team framework.

(33.64 dB PSNR, 0.94 SSIM), validating the potential of low-complexity modular pipelines for HDR restoration.

## Acknowledgments

This work was partially supported by the Alexander von Humboldt Foundation. We thank the AIM 2025 sponsors: AI Witchlabs and University of Würzburg (Computer Vision Lab).

## 4. Challenge Methods and Teams

### 4.1. ToneMapper: Boosting Inverse Tone Mapping via Regularization Training

**General method description.** The proposed network architecture is mainly based on NAFNet [10], which fuses multi-scale image information through a series of convolutional layers and skip connections to process LDR images into HDR images [47, 48, 50, 51]. It should be noted that inspired by EEDTP [49], we use regularized enhancement training to improve the performance of ordinary restoration models, which greatly improves the image processing effect. Please see Figure 2.

**Total method complexity.**

- Number of parameters = 27.18M
- FLOPs = 4.84G
- GPU memory consumption: A GTX1080 is sufficient

**Training strategy.** Inverse Tone Mapping aims to reconstruct a high dynamic range from a low dynamic range input image. Due to the complexity of dynamic scenes, LDR images with different exposures have the same complex degradation conditions, which poses a severe test for the generalization of the image restoration network. Therefore, we used the generalization-enhanced regularization method in EEDTP [49] to promote better restoration of HDR effects.

Our training process is divided into three stages:

1. We adopt the Adam optimizer with a batch size of 100 and the patch size of  $64 \times 64$ . The initial learning rate is  $4 \times 10^{-4}$  and changes with Cosine Annealing scheme, including 1000 epochs in total. The first stage is performed on the NVIDIA 4090D device. We obtain the best model at this stage as the initialization of the second stage.

2. We adopt the Adam optimizer with a batch size of 50 and the patch size of  $128 \times 128$ . The initial learning rate is  $4 \times 10^{-5}$  and changes with Cosine Annealing scheme, including 300 epochs in total. The second stage is performed on the NVIDIA 4090D device and uses gradient accumulation. We obtain the best model at this stage as the initialization of the next stage.
3. We adopt the SGD optimizer with a batch size of 22 and the patch size of  $256 \times 256$ . The initial learning rate is  $2 \times 10^{-5}$  and changes with Cosine Annealing scheme, including 200 epochs in total. The third stage is performed on the NVIDIA 4090D device and uses gradient accumulation.

**Testing strategy.** During the test time, we adopt the model after fine-tuning to get the best performance. Moreover, we utilize input-ensemble strategy to obtain the best results. We test the model on NVIDIA 4090D.

*Results of the comparison to other approaches.* We tested the previous SOTA models HirFormer [47], EvenFormer [48], AALN [51], ILAWR [50], and EEDTP [49] in motion deblurring. HirFormer and EvenFormer have low training efficiency due to high video memory usage, while AALN and ILAWR cannot achieve optimal performance.

*Experimental results.* In quantitative results, our approach achieves the highest PSNR on the AIM 2025 Inverse Tone Mapping Challenge test dataset.

**Best scores for development/testing:**

- PU21-PSNR: 34.58 / 34.49
- PU21-SSIM: 0.95 / 0.95

## 4.2. HDRer: Deep High Dynamic Range Imaging via Dynamic Scenes Generation

**General method description.** The proposed network architecture is mainly based on NAFNet [10], which fuses multi-scale image information through a series of convolutional layers and skip connections to process LDR images into HDR images [47, 48, 50, 51]. It should be noted that inspired by AALN [51], we use Diffusion to generate more low-dynamic scene images to enhancement training to improve the performance of ordinary restoration models, which greatly improves the image processing effect. Please see Figure 4 and Figure 3.

**Total method complexity.**

- Number of parameters = 15.51M
- FLOPs = 2.80G
- GPU memory consumption: A GTX1080 is sufficient

**Training strategy.** Our training process is divided into three stages:

1. We adopt the Adam optimizer with a batch size of 100 and the patch size of  $64 \times 64$ . The initial learning rate is  $4 \times 10^{-4}$  and changes with Cosine Annealing scheme, including 1000 epochs in total. The first stage is performed on the NVIDIA 4090D device. We obtain the

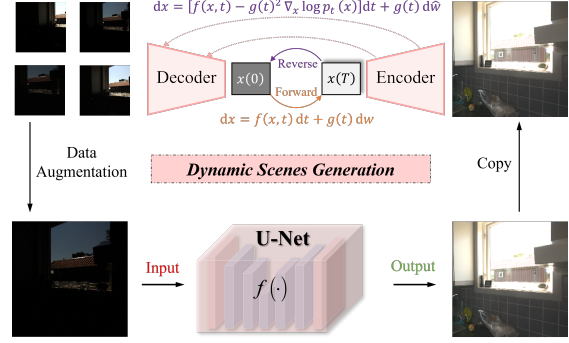


Figure 3. HDRer's team dynamic scenes generation.

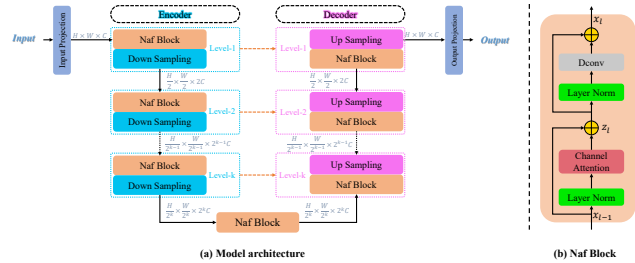


Figure 4. HDRer's team framework.

best model at this stage as the initialization of the second stage.

2. We adopt the Adam optimizer with a batch size of 50 and the patch size of  $128 \times 128$ . The initial learning rate is  $4 \times 10^{-5}$  and changes with Cosine Annealing scheme, including 300 epochs in total. The second stage is performed on the NVIDIA 4090D device and uses gradient accumulation. We obtain the best model at this stage as the initialization of the next stage.
3. We adopt the SGD optimizer with a batch size of 22 and the patch size of  $256 \times 256$ . The initial learning rate is  $2 \times 10^{-5}$  and changes with Cosine Annealing scheme, including 200 epochs in total. The third stage is performed on the NVIDIA 4090D device and uses gradient accumulation.

**Testing strategy.** During the test time, we adopt the model after fine-tuning to get the best performance. Moreover, we utilize input-ensemble strategy to obtain the best results. We test the model on NVIDIA 4090D.

*Results of the comparisons to other approaches results.* We tested the previous SOTA models HirFormer [47], EvenFormer [48], AALN [51], ILAWR [50], and EEDTP [49] in motion deblurring. HirFormer and EvenFormer have low training efficiency due to high video memory usage, while AALN and ILAWR cannot achieve optimal performance.

*Experimental results.* In quantitative results, our approach achieves the 2nd highest PSNR on the AIM 2025 Inverse Tone Mapping Challenge test dataset.

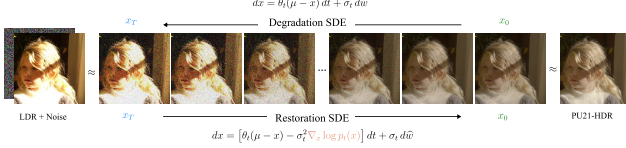


Figure 5. Pipeline of *LiU.CGIP*'s solution: The LDR input is processed through the restoration SDE to generate a PU21-HDR representation, which is subsequently decoded to produce the final HDR output.

#### Best scores for development/testing:

- PU21-PSNR: 33.09 / 34.39
- PU21-SSIM: 0.93 / 0.95

### 4.3. LiU.CGIP: What Makes Inverse Tone Mapping Hard? An Empirical Study of Error Patterns and Perceptual Challenges

**General method description.** We employ Refusion [53], a score-based diffusion model as the backbone of our solution for the AIM 2025 ITM Challenge. Refusion is characterized by two key components. First, it adopts mean-reverting stochastic differential equations (SDE) [52], a specialized formulation of the diffusion SDE [70], which requires both the noise and the degraded image as inputs. Second, instead of the commonly used U-Net architecture [65], Refusion utilizes a modified NAFBlock [11] as its backbone, offering improved performance and less computational cost in image reconstruction tasks. As illustrated in Figure 5, we first map HDR images to the PU21 space [3], then add noise to their corresponding LDR counterparts in order to reconstruct PU21-HDR. Finally, these PU21-HDR representations are decoded back to HDR images. Similar to other score-based diffusion models, Refusion employs a forward degradation process governed by an SDE:

$$dx = \theta_t(\mu - x) dt + \sigma_t dw. \quad (1)$$

Given this forward SDE, the corresponding backward restoration SDE is formulated as

$$dx = [\theta_t(\mu - x) - \sigma_t^2 \nabla_x \log p_t(x)] dt + \sigma_t d\hat{w}. \quad (2)$$

To train the model, Refusion minimizes the following objective function

$$J_\gamma(\phi) := \sum_{i=1}^T \gamma_i \mathbb{E}[\|x_{i-1} - x_{i-1}^*\|], \quad (3)$$

where  $x_{i-1}^*$  is derived by [53] via maximum likelihood estimation, and  $x_{i-1}$  is obtained from Eq. (2). The score function  $\nabla_x \log p_t(x)$  is approximated using a modified NAFNet architecture parameterized by  $\phi$ . The weights  $\gamma_1, \dots, \gamma_T$  are positive scalars that balance the contributions of each timestep. For further details, we refer the

reader to [53]. However, empirical results show that using the  $\ell_1$  loss yields better performance than the  $\ell_2$  loss. Therefore, we incorporate an additional SSIM-based regularization term to formulate the total score-matching loss as:

$$J_\gamma(\phi) := \sum_{i=1}^T \gamma_i \mathbb{E}[\|x_{i-1} - x_{i-1}^*\| + \lambda \cdot \ell_{\text{SSIM}}(x_{i-1}, x_{i-1}^*)], \quad (4)$$

where  $\ell_{\text{SSIM}}(x, \hat{x}) = 1 - \text{SSIM}(x, \hat{x})$  and  $\lambda$  is a positive weight.

**Total method complexity.** The final model, Refusion, contains 131.4M parameters. For a  $512 \times 512$  input, the computational cost is 253.6G FLOPs, with an average runtime of approximately 6 seconds on a single A100 GPU.

**Training strategy.** We utilize additional data from the HDRCNN dataset [22]. Detailed statistics are provided in Table 3. For generating the corresponding LDR images, we use HDRCNN's virtual camera simulation to synthesize 104K image pairs at a resolution of  $256 \times 256$ . The simulation includes random cropping, camera response curve mapping, exposure clipping, and Gaussian noise injection, and then normalization to  $[0, 1000]$ . Further implementation details are available in Appendix A of HDRCNN [22].

We first train the model solely on the HDRCNN dataset [22]. The training uses the LION optimizer [12] with an initial learning rate of  $4 \times 10^{-5}$ . Cosine annealing is applied without warm-up. The model is trained for 700,000 iterations with a batch size of 8, taking approximately 2.5 days on a single NVIDIA A100 GPU. We then fine-tune the pretrained model jointly on both the HDRCNN dataset and the official AIM Inverse Tone Mapping Challenge dataset for another 700,000 iterations, using a reduced learning rate of  $1 \times 10^{-5}$ . All models are trained from scratch without using any external pretrained weights. For the diffusion process, we use a cosine noise schedule with 100 discretized time steps.

**Testing strategy.** We do not employ any test-time augmentation. During inference, we simply run the backward restoration SDE to reconstruct PU21-HDR images, which are then decoded to linear HDR.

**Quantitative Results.** Our qualitative results on the test set are summarized in Table 2. Training with additional data significantly improves both PU21-PSNR and PU21-SSIM metrics. Note that we did not submit other model variants to the test leaderboard, therefore, further ablation studies would require access to ground truth data for the test set.

**Qualitative Results.** As shown in Figure 6, we visualize error maps across different scenarios. Most noticeable errors appear in overexposed regions, particularly in the second and third rows. The last row highlights missing details in underexposed areas, such as completely dark buildings.

Method	PU21-PSNR $\uparrow$	PU21-SSIM $\uparrow$
Refusion	33.62	0.9371
Refusion + extra data	34.33	0.9421

Table 2. *LiU\_CGIP*'s ablation on PU21 metrics.

Name	Source	Size
EMPA	<a href="http://www.empamedia.ethz.ch/hdrdatabase/index.php">http://www.empamedia.ethz.ch/hdrdatabase/index.php</a>	33
HDReye	<a href="http://mmpg.epfl.ch/hdr-eye">http://mmpg.epfl.ch/hdr-eye</a>	46
Fairchild	<a href="http://rit-mcsl.org/fairchild/HDRFS/HDRthumbs.html">http://rit-mcsl.org/fairchild/HDRFS/HDRthumbs.html</a>	106
Ward	<a href="http://www.anywhere.com/gward/hdrenc/pages/originals.html">http://www.anywhere.com/gward/hdrenc/pages/originals.html</a>	33
Stanford	<a href="http://scarlet.stanford.edu/~brian/hdr/hdr.html">http://scarlet.stanford.edu/~brian/hdr/hdr.html</a>	91
MCSL	<a href="http://www.cis.rit.edu/research/mcs12/icom/hdr/rit_hdr/">http://www.cis.rit.edu/research/mcs12/icom/hdr/rit_hdr/</a>	74
Funt	<a href="http://www.cs.sfu.ca/~colour/data/funt_hdr/#DATA">http://www.cs.sfu.ca/~colour/data/funt_hdr/#DATA</a>	112
Boitard	<a href="https://people.irisa.fr/Ronan.Boitard/">https://people.irisa.fr/Ronan.Boitard/</a>	7 sequences
MPI	<a href="http://resources.mpi-inf.mpg.de/hdr/video/">http://resources.mpi-inf.mpg.de/hdr/video/</a>	2 sequences
DML-HDR	<a href="http://dml.ece.ubc.ca/data/DML-HDR/">http://dml.ece.ubc.ca/data/DML-HDR/</a>	5 sequences
HDR book	Images accompanying the HDR book by Reinhard <i>et al.</i> [2005].	327
JPEG-XT	Images used in the evaluation by Mantiuk <i>et al.</i> [2016].	174
Stuttgart	<a href="https://hdr-2014.hdm-stuttgart.de/">https://hdr-2014.hdm-stuttgart.de/</a>	33 sequences
LiU HDRV	<a href="http://hdrv.org">http://hdrv.org</a>	10 sequences
Sequences	Miscellaneous sequences	10 sequences
Probes	Miscellaneous lightprobes/panoramas	12
Images	Miscellaneous images	113
<b>Total</b>	-	<b>4392 images</b>

Table 3. *LiU\_CGIP*'s extra HDR datasets and their sources. We simulated LDR data the same way as in HDRCNN [22].

To better understand the model behavior, we perform a statistical error analysis. We randomly sample 100 images from the training set and compare LDR intensity values with the corresponding prediction errors. As shown in Figure 7a, we observe a general trend: prediction error tends to increase slightly with intensity, and a concentration of high errors is visible near intensity value 255.

We define the top 15% of pixel intensities as the saturated region and analyze their error distribution in Figure 7b. Compared to the full image distribution, the saturated regions show a distinct pattern with more high-error outliers.

Additional visual results are shown in Figure 8. For example, in the first row, the reconstruction of an overexposed color chart exhibits unrealistic artifacts. These findings suggest that the most challenging aspect of ITM lies in regions with missing information. Large-scale inpainting models may help address these limitations. Moreover, saturated regions are difficult to evaluate using traditional objective metrics such as PU21-PSNR and PU21-SSIM, which may necessitate the development of more perceptually aligned evaluation methods.

#### Best scores for development/testing:

- PU21-PSNR: 34.51/34.33
- PU21-SSIM: 0.94/0.94

#### 4.4. NJ Challenger: Learning to Reverse the Camera Pipeline by PyTorch

**General method description.** Our method is a novel approach for single-image High Dynamic Range (HDR) reconstruction by learning to reverse the camera pipeline. Instead of directly mapping a Low Dynamic Range (LDR) im-

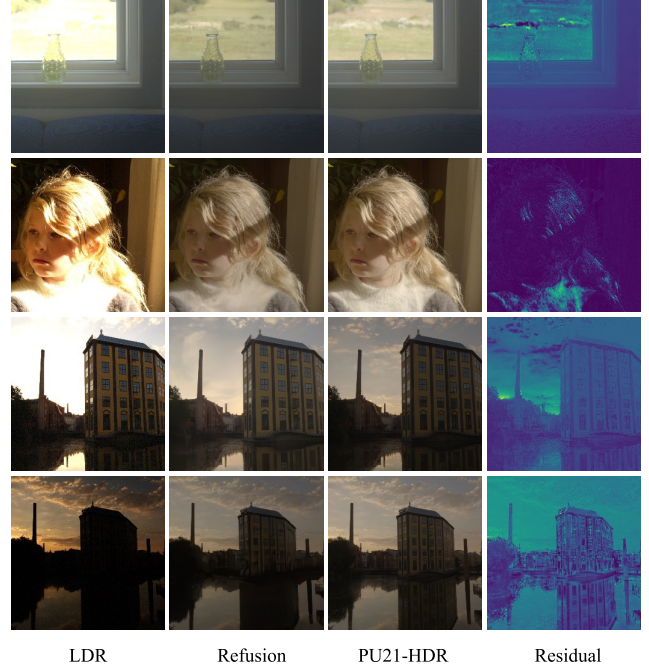
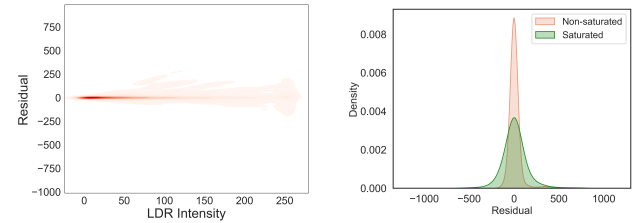


Figure 6. *LiU\_CGIP* error map: Absolute residual between prediction and groundtruth PU21-HDR.



(a) LDR intensity v.s. HDR error (b) Saturated v.s. non-saturated

Figure 7. *LiU\_CGIP*'s error distribution: (a) Joint 2D distribution of input LDR intensity and prediction error. (b) Error distribution on saturated and non-saturated area, 15% percentile. Both figures are calculated on 100 randomly sampled images from training set.

age to an HDR image, the method decomposes the problem into three sub-tasks, each handled by a specialized neural network [45]:

- Dequantization-Net: Restores missing details caused by quantization (e.g., banding artifacts in underexposed regions). The network is U-Net architecture with skip connections to reduce quantization artifacts.
- Linearization-Net: Estimates the inverse Camera Response Function (CRF) to convert the non-linear LDR image to a linear irradiance map. This part is ResNet-18 backbone with edge/histogram features and monotonicity constraints for CRF estimation.
- Hallucination-Net: Predicts missing content in overexposed regions by generating positive residuals. We use

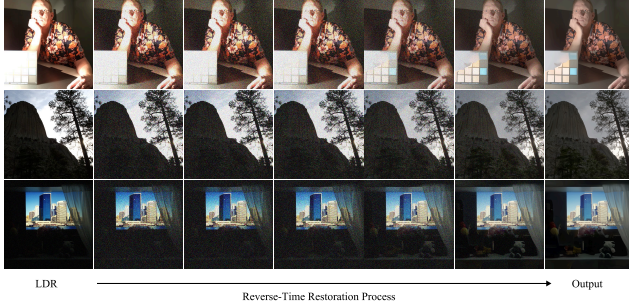


Figure 8. *LiU\_CGIP*'s more results. Samples from development/validation datasets, image id from top to bottom: `im_000045_000002.jpg`, `im_000029_000002.jpg` and `im_000057_000001.jpg`.

Encoder (VGG16) and Decoder with resize-convolution layers to avoid checkerboard artifacts, predicting positive residuals for over-exposed regions.

The input LDR Image will be processed through three sequential networks. First, the LDR will be inputted into the Dequantization-Net to get a detailed dequantized LDR. Then, Linearization-Net can estimate the inverse, which converts dequantized LDR to linear image. Finally, Hallucination-Net will restore missing content in overexposed regions, and the HDR image will be outputted.

**Total method complexity.** The number of parameters of Dequantization-Net is 1.99M. The number of parameters of Hallucination-Net is 24.57M. The number of parameters of Linearization-Net is 1.2M.

**Training strategy.** The training is on one 24G NVIDIA GeForce RTX 4060 for a total of 10 days. It takes 3 days to train the Dequantization-Net and also takes 3 days to train the Linearization-Net. And we spend 4 days training the Hallucination-Net. The learning rate scheduler is the cosine annealing scheduler, and the optimizer is the adaptive moment estimation. The learning rate is set to  $1 \times 10^{-4}$ . And we train Dequantization-Net for 10K iterations with batch size 64, Linearization-Net for 10K iterations with batch size 64, and Hallucination-Net for 10K iterations with batch size 32. Then we use different losses for each network.

**Dequantization-Net:** Trained with  $l_2$  loss between dequantized output and ground-truth non-linear image.

**Linearization-Net:** Uses edge/histogram features and enforces monotonicity constraints. The loss combines  $l_2$  for linear image and CRF reconstruction.

**Hallucination-Net:** Optimized with log- $l_2$  loss (for highlight regions), perceptual loss (VGG features on tonemapped images), and TV loss (for smoothness).

Training data is the official training set: Approximately 19,000 LDR-HDR image pairs at a resolution of  $256 \times 256$ , collected from various public HDR datasets. The LDR counterparts are synthesized using a range of exposure set-

tings, quantization effects, and noise patterns. We never use any additional training data.

We use pretrained VGG16 and VGG16-places-365 in our Hallucination-Net, VGG16-places-365 is used to initialize the model from the pretrained model, and VGG16 is for perceptual loss. We also use pretrained Crfnets weights to initialize the model for our Linearization-Net.

**Experimental results.** According to official benchmark, the evaluation uses perceptual quality metrics designed for HDR data: 100 LDR inputs will be provided during the final testing phase. The HDR ground truths will remain hidden for unbiased evaluation.

**Best scores for development/testing:**

- PU21-PSNR: 29.83 / 29.22
- PU21-SSIM: 0.85 / 0.85

#### 4.5. UESTC-ITM: Towards High-Quality Inverse Tone Mapping with Conditional Flow Matching

**General method description.** *Motivation:* Single-image inverse tone mapping (ITM) remains an ill-posed and underconstrained problem, particularly in the presence of saturated highlights, crushed shadows, and quantization artifacts common in legacy LDR imagery. Prior regression-based solutions often fail to hallucinate plausible content in severely clipped or saturated regions, leading to poor detail restoration in reconstructed HDR images. On the other hand, recent advances in generative models have demonstrated strong capabilities in synthesizing perceptually convincing details for various image restoration tasks.

*Method Overview:* In this challenge, we propose a dual branch framework, namely ITMFlow, to tackle the inverse tone mapping (ITM) problem using conditional flow matching (CFM) [73], a principled generative modeling framework that learns to reconstruct HDR images conditioned on the LDR input. By modeling the transformation between LDR and HDR distributions, the CFM branch effectively restores structural and textural details even in highly ill-posed regions. To complement the generative pathway and ensure metric-aligned fidelity, ITMFlow is designed as a dual-branch architecture, where a second branch employs a hybrid CNN + Vision Transformer (ViT) design. Specifically, we adopt NAFNet [11] as a lightweight yet expressive CNN backbone for local detail recovery, while ViT layers [20] capture global contextual information. This deterministic branch is optimized using PU-based metrics to ensure radiometric consistency and quantitative performance. Finally, the outputs of both branches are fused by averaging, effectively combining the perceptual richness of the generative model with the accuracy of deterministic regression. This strategy leads to robust and detail-preserving HDR reconstructions across a wide range of degradations. The overall pipeline of the proposed ITMFlow is illustrated in Fig. 9.

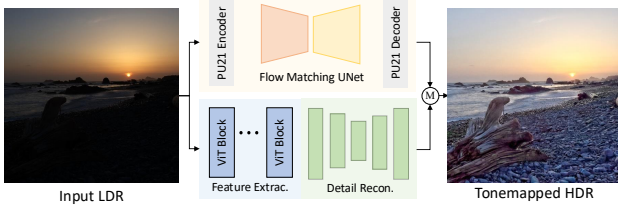


Figure 9. Overview of the *UESTC-ITM*'s proposed ITMFlow. The pipeline comprises two branches: a conditional flow matching (CFM) branch that generates HDR predictions conditioned on the input LDR and noise, enabling robust detail recovery in ill-posed regions; and a ViT+CNN regression branch that ensures high-fidelity reconstruction through global context modeling and local refinement. The final HDR output is obtained by averaging the predictions from both branches.

#### Total method complexity.

- Parameters: 69.79M (Flow Matching branch: 29.74M, ViT+CNN branch: 40.05M)
- FLOPs: 324.98G (Flow Matching branch: 249.41G, ViT+CNN branch: 75.57G)
- Runtime: 1.41s on NVIDIA RTX 4090 GPU for a single image of size  $512 \times 512$ .

**Training strategy.** The proposed ITMFlow framework adopts a decoupled training strategy, where the two branches are trained independently. The flow matching branch is trained to reconstruct the PU21-encoded HDR representation. The model learns to predict the conditional velocity field that guides the transformation from noisy LDR inputs to the target PU21-encoded HDR distribution. During inference, the output is passed through a PU21 decoder to obtain the final HDR image. The hybrid ViT+CNN branch is trained in a supervised manner to directly regress the HDR output from the LDR input. At test time, both branches produce independent HDR predictions, which are averaged pixel-wise to obtain the final output.

Note that we train our model from scratch: we only used the provided data to train and validate our model, and no additional data has been used.

**Experimental results.** Figure 10 illustrates the reconstructed HDR results from ViT and our ITMFlow. Compared to the ViT, ITMFlow achieves better detail reconstruction in overexposed regions and produces results with higher visual consistency and perceptual fidelity.

#### Best scores for development/testing:

- PU21-PSNR: 33.6 / 34.06
- PU21-SSIM: 0.94 / 0.94

### 4.6. Jowgik: DITM

**General method description.** DITM is a modular neural architecture for reconstructing HDR images from LDR sRGB inputs, see Figure 11. It consists of four main stages: noise-aware bit recovery, learnable exposure aggregation,

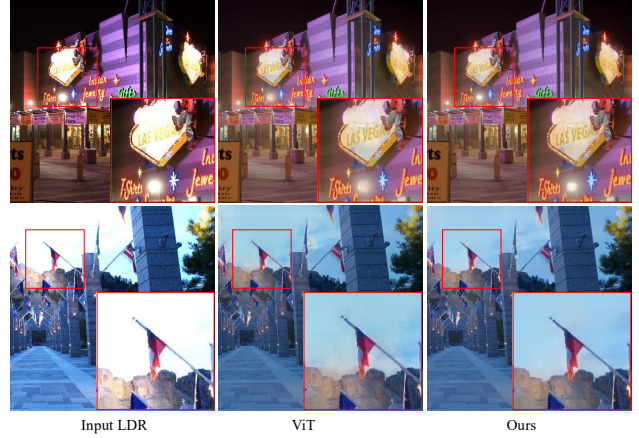


Figure 10. Illustration of the reconstructed HDR results of *UESTC-ITM*.

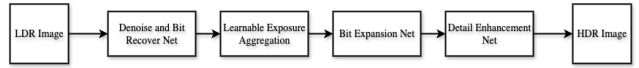


Figure 11. *Jowgik*'s pipeline.

progressive HDR expansion, and final refinement. The development was influenced by SingleHDR[45] methodology, which provided valuable insights for our architectural design and loss function formulation.

The main step of the pipeline, given an input  $\mathbf{x}_{\text{srgb}} \in \mathbb{R}^{3 \times H \times W}$ , are:

1. Convert to linear RGB using sRGB function:

$$\mathbf{x}_{\text{lin}} = \begin{cases} \frac{\mathbf{x}_{\text{srgb}}}{12.92}, & \mathbf{x}_{\text{srgb}} \leq 0.04045 \\ \left( \frac{\mathbf{x}_{\text{srgb}} + 0.055}{1.055} \right)^{2.4}, & \text{otherwise} \end{cases} \quad (5)$$

2. Denoise and recover bit details using *BitRecoverNet*.
3. Expand dynamic range progressively using *BitExpansionNet*.
4. Refine spatial details using *DetailEnhancementNet*.

*BitRecoverNet*. This module removes quantization noise and reconstructs latent HDR content.

Dilated-conv stack estimates a spatial noise map:

$$\hat{\mathbf{n}} = f_{\text{noise}}(\mathbf{x}_{\text{lin}}). \quad (6)$$

A residual branch adaptively denoises the signal:

$$\hat{\mathbf{x}} = \mathbf{x}_{\text{lin}} \cdot (1 + \tanh(\beta) \cdot f_{\text{denoise}}([\mathbf{x}_{\text{lin}}, \hat{\mathbf{n}}])). \quad (7)$$

The input is decomposed into under-, mid-, and over-exposed components.

First, blurred luminance is computed as:

$$L = 0.2126R + 0.7152G + 0.0722B \quad (8)$$

$$\bar{L} = L * k, \quad k = \text{mean\_kernel}, \quad (9)$$

then, it is softmax-normalized thresholds:

$$\{\tau_i\}_{i=1}^2 = \text{cumsum}(\text{softmax}(\theta)). \quad (10)$$

Finally, the exposure masks are computed as:

$$M_{\text{under}} = 1 - \sigma(\alpha(\bar{L} - \tau_1)) \quad (11)$$

$$M_{\text{mid}} = \sigma(\alpha(\bar{L} - \tau_1)) - \sigma(\alpha(\bar{L} - \tau_2)) \quad (12)$$

$$M_{\text{over}} = \sigma(\alpha(\bar{L} - \tau_2)). \quad (13)$$

At this point, weighted fusion of masked images is computed as:

$$\mathbf{x}_{\text{under}} = \hat{\mathbf{x}} \cdot M_{\text{under}} \quad \mathbf{x}_{\text{mid}} = \hat{\mathbf{x}} \cdot M_{\text{mid}} \quad \mathbf{x}_{\text{over}} = \hat{\mathbf{x}} \cdot M_{\text{over}} \quad (14)$$

$$\mathbf{w} = \text{softmax}(f_w([\mathbf{x}_{\text{under}}, \mathbf{x}_{\text{mid}}, \mathbf{x}_{\text{over}}])). \quad (15)$$

$$\mathbf{x}_{\text{fused}} = \sum_i \mathbf{w}_i \cdot \mathbf{x}_i. \quad (16)$$

The final enhancement is applied via residual projection:

$$\mathbf{x}_{\text{deq}} = \mathbf{x}_{\text{fused}} \cdot (1 + \sigma(\alpha) \cdot f_{\text{res}}(\mathbf{x}_{\text{fused}})). \quad (17)$$

*BitExpansionNet* expands the dequantized image to full HDR via a multi-scale encoder-fusion-decoder architecture.

Its encoder has hierarchical features defined as:

$$x_1 = f_1(\mathbf{x}_{\text{deq}}) \quad x_2 = f_2(x_1) \quad x_3 = f_3(x_2). \quad (18)$$

Each level uses attention-weighted feature fusion:

$$A = \sigma(f_{\text{eca}}(\text{avgpool}(x))) \cdot \sigma(f_{\text{spa}}(\text{mean}_c(x))) \quad (19)$$

$$x_{\text{fused}} = f_{\text{conv}}(x) \cdot A. \quad (20)$$

HDR predictions are generated at each scale with skip connections:

$$f_1, o_1 = \text{proj}_1(x_{\text{fused}}, \text{None}, \mathbf{x}_{\text{deq}}) \quad (21)$$

$$f_2, o_2 = \text{proj}_2(f_1, f_1, o_1) \quad (22)$$

$$f_3, o_3 = \text{proj}_3(f_2, f_2, o_2). \quad (23)$$

*DetailEnhancementNet*. A shallow U-Net structure further enhances spatial and contrast details of the final HDR prediction.

Skip features are aggregated across five encoder levels and progressively upsampled:

$$\mathbf{y}_{\text{hdr}} = o_3 \cdot (1 + \sigma(\alpha) \cdot f_{\text{enhance}}(o_3)) \quad (24)$$

### Total method complexity.

- Number of parameters: 1.97M
- FLOPs: 25.64G (for standard input resolution)
- Number of activations: 85.29M

- Number of Conv2d layers: 81
- GPU memory consumption: Efficient processing with adaptive padding for arbitrary resolutions
- Runtime: Successfully tested on resolutions including  $640 \times 480$ ,  $321 \times 241$  with robust handling of arbitrary input dimensions
- Model initialization: Kaiming initialization applied to all layers for stable training

**Training strategy.** During training, the model outputs all intermediate results  $[x_{\text{denoised}}, x_{\text{deq}}, o_1, o_2, o_3, \text{hdr}]$ , enabling supervision at multiple stages of the pipeline for improved gradient flow and feature learning. The progressive HDR expansion stages ( $o_1, o_2, o_3$ ) receive weighted supervision with increasing importance for later stages.

**Composite Loss Function.** The training employs a sophisticated composite loss combining multiple terms for comprehensive supervision:

Core reconstruction terms:

- **Reconstruction Loss:** Weighted  $\mu$ -law compressed domain L1 loss across all HDR stages, with progressively increasing weights for later stages:

$$L_{\text{recon}} = \sum_{i=1}^N \frac{i}{N} \cdot \|R_{\mu}(\text{pred}_i) - R_{\mu}(\text{gt})\|_1, \quad (25)$$

where the  $\mu$ -law range compressor is defined as:

$$R_{\mu}(x) = \frac{\log(1 + \mu \cdot x)}{\log(1 + \mu)} \quad \mu = 5000. \quad (26)$$

- **Linear Loss:** Direct L1 supervision on final HDR output in linear space:

$$L_{\text{linear}} = \|f(\text{input}) - \text{gt}\|_1. \quad (27)$$

- **Denoising Loss:** High-frequency denoising loss using local mean subtraction:

$$L_{\text{denoised}} = \|\text{denoised} - \text{gt}\|_1. \quad (28)$$

Perceptual quality terms:

- $L_{\text{perc}}$ : VGG16-based perceptual loss on tone-mapped outputs using `relu1_2`, `relu2_2`, `relu3_3`, `relu4_3` features.
- $L_{\text{ssim\_pu}}$ : SSIM loss in Perceptual Uniform (PU) encoding space:  $\text{PU}(x) = \frac{\log_{10}(1+c \cdot x)}{\log_{10}(1+c)}$  with  $c = 10000$ .
- $L_{\text{color}}$ : Log-chrominance consistency using three log-ratio channels (R/G, G/B, B/R) for exposure-invariant color preservation.

Advanced quality metrics:

- **Unified Patch Fidelity Loss:** Combining focal Charbonnier loss on log-luminance patches, global soft-histogram matching in log domain, and edge-aware smoothness regularization:

$$L_{\text{upf}} = L_{\text{charb}} + \alpha_{\text{hist}} L_{\text{hist}} + \beta_{\text{smooth}} L_{\text{smooth}} \quad (29)$$

From Editors: This is an approximation of PU using the  $\mu$ -law

- *Total Variation Loss*: Anisotropic total variation regularization for spatial smoothness:

$$L_{tv} = \|\nabla_h \text{pred}\|_1 + \|\nabla_v \text{pred}\|_1 \quad (30)$$

The total composite loss function is:

$$\begin{aligned} L_{\text{total}} = & L_{\text{recon}} + \alpha_{\text{perc}} L_{\text{perc}} + \gamma_{\text{ssim}} L_{\text{ssim\_pu}} \\ & + \gamma_{\text{color}} L_{\text{color}} + \gamma_{\text{tv}} L_{\text{tv}} + \lambda_{\text{linear}} L_{\text{linear}} \\ & + \alpha_{\text{denoise}} L_{\text{denoised}} + \alpha_{\text{upf}} L_{\text{upf}} \end{aligned} \quad (31)$$

Training Configuration:

- Input channels: 3 (RGB)
- Output channels: 3 (RGB)
- Base feature dimension: 32
- Pyramid levels: 3
- Loss weights:  $\alpha_{\text{perc}} = 0.1$ ,  $\gamma_{\text{ssim}} = 0.1$ ,  $\gamma_{\text{color}} = 0.05$ ,  $\lambda_{\text{linear}} = 0.1$ ,  $\alpha_{\text{denoise}} = 0.1$ ,  $\alpha_{\text{upf}} = 0.1$ ,  $\gamma_{\text{tv}} = 0.1$
- UPF parameters: patch size = 16, focal gamma = 1.5, histogram bins = 64, histogram sigma = 0.1
- Batch size: 16
- Learning rate schedule: Cosine Annealing with base LR set to  $2 \times 10^{-4}$  and annealed to  $\text{lr}_{\text{min}} = 1 \times 10^{-6}$ , and  $T = 350$  epochs
- Optimizer: Adam
- Training epochs: 350

The training pipeline incorporates standard geometric augmentations including horizontal/vertical flipping and rotations to improve model generalization and robustness to different image orientations.

The DITM model is trained from scratch without using any pretrained models (i.e., model trained from random initialization) or external methods using the PyTorch framework with standard components.

**Testing strategy.** The model evaluation employs a comprehensive testing framework that supports multiple evaluation modes and datasets. The testing protocol includes:

*Evaluation Metrics:*

- RMSE: Root Mean Square Error in linear HDR domain.
- PSNR: Peak Signal-to-Noise Ratio calculated in Perceptual Uniform (PU) encoding space for HDR-appropriate quality assessment.
- SSIM: Structural Similarity Index Measure computed in PU domain to better reflect perceptual quality differences.
- Runtime: The average inference time per image measured using CUDA events for precise GPU timing.

*Testing Protocol.* The evaluation framework supports arbitrary input resolutions through adaptive padding mechanisms, ensuring consistent processing across different image sizes. The model outputs are evaluated against ground truth in multiple domains:

- Linear HDR domain for pixel-level accuracy assessment.
- Perceptual Uniform (PU) encoded space using  $\text{PU}(x) = \frac{\log_{10}(1+10000 \cdot x)}{\log_{10}(1+10000)}$  for perceptually-relevant quality metrics

- Tone-mapped space using  $\mu$ -law compression for visualization quality evaluation.

**Best scores for development/testing:**

- PU21-PSNR: 33.3 / 33.64
- PU21-SSIM: 0.94 / 0.94

## Acknowledgments

This work was partially supported by the Alexander von Humboldt Foundation. We thank the AIM 2025 sponsors: AI Witchlabs and University of Würzburg (Computer Vision Lab).

## A. Teams and Affiliations

### AIM 2025 Inverse Tone Mapping Challenge

*Title:* AIM 2025 Inverse Tone Mapping Challenge

*Members:*

Chao Wang<sup>1,2</sup> ([winchao1984@gmail.com](mailto:winchao1984@gmail.com)),  
 Francesco Banterle<sup>3</sup> ([francesco.banterle@isti.cnr.it](mailto:francesco.banterle@isti.cnr.it)),  
 Bin Ren<sup>4,5</sup> ([bin.ren@unitn.it](mailto:bin.ren@unitn.it)),  
 Radu Timofte<sup>6</sup> ([Radu.Timofte@uni-wuerzburg.de](mailto:Radu.Timofte@uni-wuerzburg.de))

*Affiliations:*

<sup>1</sup> Max-Planck-Institut für Informatik (MPI), Germany

<sup>2</sup> Peng Cheng Laboratory, China

<sup>3</sup> ISTI-CNR, Italy

<sup>4</sup> University of Pisa, Italy

<sup>5</sup> University of Trento, Italy

<sup>6</sup> Computer Vision Lab, University of Würzburg, Germany

### ToneMapper

*Team Name:* ToneMapper

*Title:* Boosting Inverse Tone Mapping via Regularization Training

*Members:* Xin Lu (team leader, [luxion@mail.ustc.edu.cn](mailto:luxion@mail.ustc.edu.cn)),  
 Yufeng Peng, Chengjie Ge, Zhijing Sun, Ziang Zhou, Zihao Li, Zishun Liao, Qiyu Kang, Xueyang Fu, and Zheng-Jun Zha.

*Affiliations:* University of Science and Technology of China, Hefei, China

*Team website:*

<https://xueyangfu.github.io/>.

### HDRer

*Team Name:* HDRer

*Title:* Deep High Dynamic Range Imaging via Dynamic Scenes Generation

*Members:* Xin Lu (team leader, [luxion@mail.ustc.edu.cn](mailto:luxion@mail.ustc.edu.cn)),  
 Zhijing Sun, Chengjie Ge, Xingbo Wang, Kean Liu, Senyan Xu, Yang Qiu, Qiyu Kang, Xueyang Fu, and Zheng-Jun

---

From Editors: This is an approximation of PU using the  $\mu$ -law

Zha.

**Affiliations:** University of Science and Technology of China, Hefei, China

**Team website:**

<https://xueyangfu.github.io/>

## LiU\_CGIP

**Team Name:** LiU\_CGIP

**Title:** What Makes Inverse Tone Mapping Hard? An Empirical Study of Error Patterns and Perceptual Challenges

**Members:** Yifan Ding (team leader, [yifan.ding@liu.se](mailto:yifan.ding@liu.se)), Gabriel Eilertsen, and Jonas Unger.

**Affiliations:** Linköping University, Sweden

**Team website:**

<https://github.com/limchaos/Refusion-HDR.git>.

## NJ Challenger

**Team Name:** NJ Challenger

**Title:** Learning to Reverse the Camera Pipeline by PyTorch

**Members:** Zihao Wang (team leader, [wzh960045@outlook.com](mailto:wzh960045@outlook.com)), Ke Wu, and Jinshan Pan.

**Affiliations:** Nanjing University of Science and Technology, China

**Team website:**

<https://github.com/wzh960045/singhdr-torch>.

## UESTC-ITM

**Team Name:** UESTC-ITM

**Title:** Towards High-Quality Inverse Tone Mapping with Conditional Flow Matching

**Members:** Zhen Liu (team leader, [liuzhen03@std.uestc.edu.cn](mailto:liuzhen03@std.uestc.edu.cn)), Zhongyang Li, and Shuaicheng Liu.

**Affiliations:** University of Electronic Science and Technology of China (UESTC), China

**Team website:** None.

## Jowgik

**Team Name:** Jowgik

**Title:** DITM

**Members:** S. M. Nadim Uddin (team leader, [smnadimuddin@gmail.com](mailto:smnadimuddin@gmail.com)).

**Affiliations:** Deep In Sight Co., South Korea

**Team website:**

<https://github.com/SayedNadim/ITM25>.

## References

- [1] Ahmet Oğuz Akyüz, Roland Fleming, Bernhard E Riecke, Erik Reinhard, and Heinrich H Bülthoff. Do hdr displays support ldr content? a psychophysical evaluation. *ACM Transactions on Graphics (TOG)*, 26(3):38–es, 2007. 1
- [2] Pontus Andersson, Jim Nilsson, Peter Shirley, and Tomas Akenine-Möller. Visualizing errors in rendered high dynamic range images. In *Eurographics-Short Papers*, pages 25–28. Eurographics-European Association for Computer Graphics, 2021. 2
- [3] Maryam Azimi and Rafał K. Mantiuk. Pu21: A novel perceptually uniform encoding for adapting existing quality metrics for hdr. In *IEEE Picture Coding Symposium (PCS)*, 2021. 3, 6
- [4] Francesco Banterle, Patrick Ledda, Kurt Debattista, and Alan Chalmers. Inverse tone mapping. In *Proceedings of the 4th international conference on Computer graphics and interactive techniques in Australasia and Southeast Asia*, pages 349–356, 2006. 1
- [5] Francesco Banterle, Patrick Ledda, Kurt Debattista, Alan Chalmers, and Marina Bloj. A framework for inverse tone mapping. *The Visual Computer*, 23:467–478, 2007.
- [6] Francesco Banterle, Patrick Ledda, Kurt Debattista, and Alan Chalmers. Expanding low dynamic range videos for high dynamic range applications. In *Proceedings of the 24th Spring Conference on Computer Graphics*, pages 33–41, 2008. 1
- [7] Francesco Banterle, Alessandro Artusi, Kurt Debattista, and Alan Chalmers. *Advanced high dynamic range imaging*. CRC Press, 2017. 1
- [8] Francesco Banterle, Demetris Marnerides, Thomas Bashford-rogers, and Kurt Debattista. Self-supervised high dynamic range imaging: What can be learned from a single 8-bit video? *ACM Trans. Graph.*, 43(2), 2024. 1, 2
- [9] Mojtaba Bemana, Thomas Leimkühler, Karol Myszkowski, Hans-Peter Seidel, and Tobias Ritschel. Bracket diffusion: Hdr image generation by consistent ldr denoising. *Computer Graphics Forum*, 44(2), 2025. 2
- [10] Liangyu Chen, Xiaojie Chu, Xiangyu Zhang, and Jian Sun. Simple baselines for image restoration. *arXiv preprint arXiv:2204.04676*, 2022. 4, 5
- [11] Liangyu Chen, Xiaojie Chu, Xiangyu Zhang, and Jian Sun. Simple baselines for image restoration. In *Computer Vision—ECCV 2022: 17th European Conference, Tel Aviv, Israel, October 23–27, 2022, Proceedings, Part VII*, pages 17–33. Springer, 2022. 6, 8
- [12] Xiangning Chen, Chen Liang, Da Huang, Esteban Real, Kaiyuan Wang, Hieu Pham, Xuanyi Dong, Thang Luong, Cho-Jui Hsieh, Yifeng Lu, et al. Symbolic discovery of optimization algorithms. *Advances in neural information processing systems (NeurIPS)*, 2023. 6
- [13] Özgün Çiçek, Ahmed Abdulkadir, Soeren S Lienkamp, Thomas Brox, and Olaf Ronneberger. 3d u-net: learning dense volumetric segmentation from sparse annotation. In *Medical Image Computing and Computer-Assisted Intervention—MICCAI 2016: 19th International Conference, Athens, Greece, October 17-21, 2016, Proceedings, Part II 19*, pages 424–432. Springer, 2016. 1
- [14] George Ciobotariu, Florin-Alexandru Vasluiianu, Zhuyun Zhou, Nancy Mehta, Radu Timofte, et al. AIM 2025 high FPS non-uniform motion deblurring challenge report. In *Proceedings of the IEEE/CVF International Conference on Computer Vision (ICCV) Workshops*, 2025. 2

- [15] Marcos Conde, Feiran Li, Jiacheng Li, Beril Besbinar, Vlad Hosu, Daisuke Iso, Radu Timofte, et al. Real-world raw denoising using diverse cameras: AIM 2025 challenge report. In *Proceedings of the IEEE/CVF International Conference on Computer Vision (ICCV) Workshops*, 2025. 2
- [16] Marcos Conde, Bruno Longarela, Álvaro García, Radu Timofte, et al. AIM 2025 perceptual image super-resolution challenge. In *Proceedings of the IEEE/CVF International Conference on Computer Vision (ICCV) Workshops*, 2025. 2
- [17] Paul E Debevec and Jitendra Malik. Recovering high dynamic range radiance maps from photographs. In *Seminal Graphics Papers: Pushing the Boundaries, Volume 2*, pages 643–652. 2023. 1
- [18] Piotr Didyk, Rafal Mantiuk, Matthias Hein, and Hans-Peter Seidel. Enhancement of bright video features for hdr displays. In *Computer Graphics Forum*, pages 1265–1274. Wiley Online Library, 2008. 1
- [19] Sebastian Dille, Chris Careaga, and Yağız Aksoy. Intrinsic single-image hdr reconstruction. In *European Conference on Computer Vision*, pages 161–177. Springer, 2025. 1
- [20] Alexey Dosovitskiy, Lucas Beyer, Alexander Kolesnikov, Dirk Weissenborn, Xiaohua Zhai, Thomas Unterthiner, Mostafa Dehghani, Matthias Minderer, Georg Heigold, Sylvain Gelly, et al. An image is worth  $16 \times 16$  words: Transformers for image recognition at scale. In *ICLR*, 2021. 8
- [21] Andrei Dumitriu, Florin Miron, Florin Tatui, Radu Tudor Ionescu, Radu Timofte, Aakash Ralhan, Florin-Alexandru Vasluiianu, et al. In *Proceedings of the IEEE/CVF International Conference on Computer Vision (ICCV) Workshops*, 2025. 2
- [22] Gabriel Eilertsen, Joel Kronander, Gyorgy Denes, Rafał K Mantiuk, and Jonas Unger. Hdr image reconstruction from a single exposure using deep cnns. *ACM transactions on graphics (TOG)*, 36(6):1–15, 2017. 1, 3, 6, 7
- [23] Yuki Endo, Yoshihiro Kanamori, and Jun Mitani. Deep reverse tone mapping. *ACM Trans. Graph*, 36(6):1–10, 2017. 1
- [24] Mark D Fairchild. The hdr photographic survey. In *Color and imaging conference*, pages 233–238. Society of Imaging Science and Technology, 2007. 2
- [25] Jan Froehlich, Stefan Grandinetti, Bernd Eberhardt, Simon Walter, Andreas Schilling, and Harald Brendel. Creating cinematic wide gamut hdr-video for the evaluation of tone mapping operators and hdr-displays. In *Digital photography X*, pages 279–288. SPIE, 2014. 2
- [26] Paula Garrido, Marcos Conde, Jaesung Rim, Alvaro Garcia, Sunghyun Cho, Radu Timofte, et al. Efficient real-world deblurring using single images: AIM 2025 challenge report. In *Proceedings of the IEEE/CVF International Conference on Computer Vision (ICCV) Workshops*, 2025. 2
- [27] Abhishek Goswami, Aru Ranjan Singh, Francesco Banterle, Kurt Debattista, and Thomas Bashford-Rogers. Semantic aware diffusion inverse tone mapping. *arXiv preprint arXiv:2405.15468*, 2024. 2
- [28] Param Hanji, Rafał K. Mantiuk, Gabriel Eilertsen, Saghi Hajisharif, and Jonas Unger. Comparison of single image hdr reconstruction methods — the caveats of quality assessment. In *Special Interest Group on Computer Graphics and Interactive Techniques Conference Proceedings (SIGGRAPH Conference Proceedings)*, 2022. 2, 3
- [29] Gang He, Kepeng Xu, Li Xu, Chang Wu, Ming Sun, Xing Wen, and Yu-Wing Tai. Sdrtv-to-hdrtv via hierarchical dynamic context feature mapping. In *Proceedings of the 30th ACM International Conference on Multimedia*, pages 2890–2898, 2022. 2
- [30] Andrey Ignatov, Georgy Perevozchikov, Radu Timofte, et al. 4K image super-resolution on mobile NPUs: Mobile AI & AIM 2025 challenge report. In *Proceedings of the IEEE/CVF International Conference on Computer Vision (ICCV) Workshops*, 2025. 2
- [31] Andrey Ignatov, Georgy Perevozchikov, Radu Timofte, et al. Efficient learned smartphone ISP on mobile GPUs: Mobile AI & AIM 2025 challenge report. In *Proceedings of the IEEE/CVF International Conference on Computer Vision (ICCV) Workshops*, 2025. 2
- [32] Andrey Ignatov, Georgy Perevozchikov, Radu Timofte, et al. Efficient image denoising on smartphone GPUs: Mobile AI & AIM 2025 challenge report. In *Proceedings of the IEEE/CVF International Conference on Computer Vision (ICCV) Workshops*, 2025. 2
- [33] Andrey Ignatov, Georgy Perevozchikov, Radu Timofte, et al. Adapting stable diffusion for on-device inference: Mobile AI & AIM 2025 challenge report. In *Proceedings of the IEEE/CVF International Conference on Computer Vision (ICCV) Workshops*, 2025. 2
- [34] Nima Khademi Kalantari and Ravi Ramamoorthi. Deep hdr video from sequences with alternating exposures. In *Computer graphics forum*, pages 193–205. Wiley Online Library, 2019. 2
- [35] Nikolai Karetin, Ivan Molodetskikh, Dmitry Vatolin, Radu Timofte, et al. AIM 2025 challenge on robust offline video super-resolution: Dataset, methods and results. In *Proceedings of the IEEE/CVF International Conference on Computer Vision (ICCV) Workshops*, 2025. 2
- [36] Soo Ye Kim, Jihyong Oh, and Munchurl Kim. Deep sr-itm: Joint learning of super-resolution and inverse tone-mapping for 4k uhd hdr applications. In *Proceedings of the IEEE/CVF international conference on computer vision*, pages 3116–3125, 2019. 2
- [37] Soo Ye Kim, Jihyong Oh, and Munchurl Kim. Jsi-gan: Gan-based joint super-resolution and inverse tone-mapping with pixel-wise task-specific filters for uhd hdr video. In *Proceedings of the AAAI Conference on Artificial Intelligence*, pages 11287–11295, 2020. 2
- [38] Rafael Pacheco Kovaleski and Manuel M Oliveira. High-quality brightness enhancement functions for real-time reverse tone mapping. *The Visual Computer*, 25:539–547, 2009. 1
- [39] Phuoc-Hieu Le, Quynh Le, Rang Nguyen, and Binh-Son Hua. Single-image hdr reconstruction by multi-exposure generation. In *Proceedings of the IEEE/CVF winter conference on applications of computer vision*, pages 4063–4072, 2023. 1
- [40] Siyeong Lee, Gwon Hwan An, and Suk-Ju Kang. Deep chain hdri: Reconstructing a high dynamic range image from a sin-

- gle low dynamic range image. *IEEE Access*, 6:49913–49924, 2018. 1
- [41] Siyeong Lee, Gwon Hwan An, and Suk-Ju Kang. Deep recursive hdri: Inverse tone mapping using generative adversarial networks. In *proceedings of the European Conference on Computer Vision (ECCV)*, pages 596–611, 2018. 1
- [42] Yue Li, Qi Ma, Runyi Yang, Huapeng Li, Mengjiao Ma, Bin Ren, Nikola Popovic, Nicu Sebe, Ender Konukoglu, Theo Gevers, et al. Scenesplat: Gaussian splatting-based scene understanding with vision-language pretraining. In *ICCV*, 2025. 1
- [43] Bee Lim, Sanghyun Son, Heewon Kim, Seungjun Nah, and Kyoung Mu Lee. Enhanced deep residual networks for single image super-resolution. In *Proceedings of the IEEE Conference on Computer Vision and Pattern Recognition Workshops*, pages 1132–1140, 2017. 1
- [44] Guilin Liu, Fitsum A Reda, Kevin J Shih, Ting-Chun Wang, Andrew Tao, and Bryan Catanzaro. Image inpainting for irregular holes using partial convolutions. In *Proceedings of the European conference on computer vision (ECCV)*, pages 85–100, 2018. 1
- [45] Yu-Lun Liu, Wei-Sheng Lai, Yu-Sheng Chen, Yi-Lung Kao, Ming-Hsuan Yang, Yung-Yu Chuang, and Jia-Bin Huang. Single-image hdr reconstruction by learning to reverse the camera pipeline. In *Proceedings of the IEEE/CVF Conference on Computer Vision and Pattern Recognition (CVPR)*, 2020. 1, 2, 7, 9
- [46] Ze Liu, Yutong Lin, Yue Cao, Han Hu, Yixuan Wei, Zheng Zhang, Stephen Lin, and Baining Guo. Swin transformer: Hierarchical vision transformer using shifted windows. In *Proceedings of the IEEE/CVF International Conference on Computer Vision*, pages 10012–10022, 2021. 1
- [47] Xin Lu, Yurui Zhu, Xi Wang, Dong Li, Jie Xiao, Yunpeng Zhang, Xueyang Fu, and Zheng-Jun Zha. Hirformer: Dynamic high resolution transformer for large-scale image shadow removal. In *Proceedings of the IEEE/CVF Conference on Computer Vision and Pattern Recognition (CVPR) Workshops*, pages 6513–6523, 2024. 4, 5
- [48] Xin Lu, Yuanfei Bao, Jiarong Yang, Anya Hu, Jie Xiao, Kunyu Wang, Dong Li, Senyan Xu, Kean Liu, Xueyang Fu, and Zheng-Jun Zha. Evenformer: Dynamic even transformer for real-world image restoration. In *Proceedings of the Computer Vision and Pattern Recognition Conference (CVPR) Workshops*, pages 1081–1091, 2025. 4, 5
- [49] Xin Lu, Xueyang Fu, Jie Xiao, Zihao Fan, Yurui Zhu, and Zheng-Jun Zha. Elucidating and endowing the diffusion training paradigm for general image restoration. *arXiv preprint arXiv:2506.21722*, 2025. 4, 5
- [50] Xin Lu, Jie Xiao, Yurui Zhu, and Xueyang Fu. Continuous adverse weather removal via degradation-aware distillation. In *Proceedings of the Computer Vision and Pattern Recognition Conference (CVPR)*, pages 28113–28123, 2025. 4, 5
- [51] Xin Lu, Jiarong Yang, Yuanfei Bao, Zihao Fan, Anya Hu, Kunyu Wang, Jie Xiao, Xi Wang, Hongjian Liu, Xueyang Fu, and Zheng-Jun Zha. Advancing ambient lighting normalization via diffusion shadow generation. In *Proceedings of the Computer Vision and Pattern Recognition Conference (CVPR) Workshops*, pages 1070–1080, 2025. 4, 5
- [52] Ziwei Luo, Fredrik K Gustafsson, Zheng Zhao, Jens Sjölund, and Thomas B Schön. Image restoration with mean-reverting stochastic differential equations. *International Conference on Machine Learning (ICML)*, 2023. 6
- [53] Ziwei Luo, Fredrik K Gustafsson, Zheng Zhao, Jens Sjölund, and Thomas B Schön. Refusion: Enabling large-size realistic image restoration with latent-space diffusion models. In *Proceedings of the IEEE/CVF Conference on Computer Vision and Pattern Recognition Workshops (CVPRW)*, 2023. 6
- [54] Demetris Marnerides, Thomas Bashford-Rogers, Jonathan Hatchett, and Kurt Debattista. Expandnet: A deep convolutional neural network for high dynamic range expansion from low dynamic range content. In *Computer Graphics Forum*, pages 37–49. Wiley Online Library, 2018. 1
- [55] Belen Masia, Ana Serrano, and Diego Gutierrez. Dynamic range expansion based on image statistics. *Multimedia Tools and Applications*, 76:631–648, 2017. 1
- [56] Laurence Meylan, Scott Daly, and Sabine Süsstrunk. The reproduction of specular highlights on high dynamic range displays. In *IS&T/SID 14th Color Imaging Conference (CIC)*, 2006.
- [57] Laurence Meylan, Scott Daly, and Sabine Süsstrunk. Tone mapping for high-dynamic range displays. In *Human Vision and Electronic Imaging XII*, pages 370–381. SPIE, 2007. 1
- [58] Karen Panetta, Landry Kezebou, Victor Oludare, Sos Agaian, and Zehua Xia. Tmo-net: A parameter-free tone mapping operator using generative adversarial network, and performance benchmarking on large scale hdr dataset. *IEEE Access*, 9:39500–39517, 2021. 2
- [59] Allan G Rempel, Matthew Trentacoste, Helge Seetzen, H David Young, Wolfgang Heidrich, Lorne Whitehead, and Greg Ward. Ldr2hdr: on-the-fly reverse tone mapping of legacy video and photographs. *ACM transactions on graphics (TOG)*, 26(3):39–es, 2007. 1
- [60] Bin Ren, Hao Tang, Nicu Sebe, et al. Cascaded cross mlpmixer gans for cross-view image translation. In *British Machine Vision Conference (BMVC'21)*, pages 1–14. British Machine Vision Association, BMVA, 2021. 2
- [61] Bin Ren, Yahui Liu, Yue Song, Wei Bi, Rita Cucchiara, Nicu Sebe, and Wei Wang. Masked jigsaw puzzle: A versatile position embedding for vision transformers. In *CVPR*, pages 20382–20391, 2023. 1
- [62] Bin Ren, Yawei Li, Jingyun Liang, Rakesh Ranjan, Mengyuan Liu, Rita Cucchiara, Luc V Gool, Ming-Hsuan Yang, and Nicu Sebe. Sharing key semantics in transformer makes efficient image restoration. *Advances in Neural Information Processing Systems*, 37:7427–7463, 2024. 1
- [63] Bin Ren, Hang Guo, Lei Sun, Zongwei Wu, Radu Timofte, and Yawei Li. The tenth ntire 2025 efficient super-resolution challenge report. In *Proceedings of the Computer Vision and Pattern Recognition Conference*, pages 917–966, 2025. 1
- [64] Robin Rombach, Andreas Blattmann, Dominik Lorenz, Patrick Esser, and Björn Ommer. High-resolution image synthesis with latent diffusion models. In *Proceedings of the IEEE/CVF conference on computer vision and pattern recognition*, pages 10684–10695, 2022. 2

- [65] Olaf Ronneberger, Philipp Fischer, and Thomas Brox. U-net: Convolutional networks for biomedical image segmentation. In *Medical image computing and computer-assisted intervention (MICCAI)*, 2015. 6
- [66] Nickolay Safonov, Mikhail Rakhmanov, Dmitriy Vatolin, Radu Timofte, et al. AIM 2025 challenge on screen-content video quality assessment: Methods and results. In *Proceedings of the IEEE/CVF International Conference on Computer Vision (ICCV) Workshops*, 2025. 2
- [67] Marcel Santana Santos, Tsang Ing Ren, and Nima Khademi Kalantari. Single image hdr reconstruction using a cnn with masked features and perceptual loss. *arXiv preprint arXiv:2005.07335*, 2020. 1
- [68] Konstantin Shmelkov, Cordelia Schmid, and Karteek Alahari. How good is my gan? In *Proceedings of the European conference on computer vision (ECCV)*, pages 213–229, 2018. 2
- [69] Karen Simonyan and Andrew Zisserman. Very deep convolutional networks for large-scale image recognition. *arXiv preprint arXiv:1409.1556*, 2014. 1
- [70] Yang Song, Jascha Sohl-Dickstein, Diederik P Kingma, Abhishek Kumar, Stefano Ermon, and Ben Poole. Score-based generative modeling through stochastic differential equations. In *International Conference on Learning Representations (ICLR)*, 2021. 6
- [71] Hao Tang, Bin Ren, Pingping Wu, and Nicu Sebe. Hierarchical cross-attention network for virtual try-on. *IEEE Transactions on Multimedia*, 2025. 2
- [72] Steven Tel, Zongwei Wu, Yulun Zhang, Barthélemy Heyrman, Cédric Démonceaux, Radu Timofte, and Dominique Ginjac. Alignment-free hdr deghosting with semantics consistent transformer. *arXiv preprint arXiv:2305.18135*, 2023. 2
- [73] Alexander Tong, Kilian Fatras, Nikolay Malkin, Guillaume Huguët, Yanlei Zhang, Jarrid Rector-Brooks, Guy Wolf, and Yoshua Bengio. Improving and generalizing flow-based generative models with minibatch optimal transport. *arXiv preprint arXiv:2302.00482*, 2023. 8
- [74] Chao Wang, Ana Serrano, Xingang Pan, Bin Chen, Karol Myszkowski, Hans-Peter Seidel, Christian Theobalt, and Thomas Leimkühler. Glowgan: Unsupervised learning of hdr images from ldr images in the wild. In *Proceedings of the IEEE/CVF International Conference on Computer Vision*, pages 10509–10519, 2023. 2
- [75] Chao Wang, Francesco Banterle, Bin Ren, Radu Timofte, et al. AIM 2025 challenge on inverse tone mapping report: Methods and results. In *Proceedings of the IEEE/CVF International Conference on Computer Vision (ICCV) Workshops*, 2025. 2
- [76] Chao Wang, Zhihao Xia, Thomas Leimkühler, Karol Myszkowski, and Xuaner Zhang. Lediff: Latent exposure diffusion for hdr generation. In *Proceedings of the Computer Vision and Pattern Recognition Conference*, pages 453–464, 2025. 1, 2
- [77] Weihao Xia, Yulun Zhang, Yujiu Yang, Jing-Hao Xue, Bolei Zhou, and Ming-Hsuan Yang. Gan inversion: A survey. *IEEE transactions on pattern analysis and machine intelligence*, 45(3):3121–3138, 2022. 2
- [78] Alexander Yakovenko, George Chakvetadze, Ilya Khrapov, Maksim Zhelezov, Dmitry Vatolin, Radu Timofte, et al. AIM 2025 low-light raw video denoising challenge: Dataset, methods and results. In *Proceedings of the IEEE/CVF International Conference on Computer Vision (ICCV) Workshops*, 2025. 2
- [79] Hanning Yu, Wentao Liu, Chengjiang Long, Bo Dong, Qin Zou, and Chunxia Xiao. Luminance attentive networks for hdr image and panorama reconstruction. In *Computer Graphics Forum*, pages 181–192. Wiley Online Library, 2021. 1
- [80] Ning Zhang, Yuyao Ye, Yang Zhao, and Ronggang Wang. Revisiting the stack-based inverse tone mapping. In *Proceedings of the IEEE/CVF Conference on Computer Vision and Pattern Recognition*, pages 9162–9171, 2023. 1